Brainless Bodies: Controlling the Development and Behavior of Multicellular Animats by Gene Regulation and Diffusive Signals

M. Joachimczak[1], T. Kowaliw[2], R. Doursat[2,3], and B. Wróbel[1,4,5]

[1]Systems Modeling Laboratory, IO PAN, Sopot, Poland
[2]Institut des Systèmes Complexes Paris Ile-de-France (ISC-PIF), CNRS, Paris, France
[3]Research Group in Biomimetics (GEB), Universidad de Málaga, Spain
[4]Evolutionary Systems Laboratory, Uniwersytet im. Adama Mickiewicza, Poznań, Poland
[5]Institut für Neuroinformatik, Universität & ETH Zürich, Switzerland

Abstract

We present a model of parallel co-evolution of development and motion control in soft-bodied, multicellular animats without neural networks. Development is guided by an artificial gene regulatory network (GRN), with real-valued expression levels, contained in every cell. Embryos develop within a simulated physics environment and are converted into animat structures by connecting neighboring cells through elastic springs. Outer cells, which form the external envelope, are affected by drag forces in a fluid-like environment. Both the developmental program and locomotion controller are encoded into a single genomic sequence, which consists of regulatory regions and genes expressed into transcription factors and morphogens. We apply a genetic algorithm to evolve individuals able to swim in the simulated fluid, where the fitness depends on distance traveled during the evaluation phase. We obtain various emergent morphologies and types of locomotion, some of them showing the use of rudimentary appendages. An analysis of the selected evolved controllers is provided.

Introduction

The raison d'etre of the nervous systems is to allow for controllable and adaptable movement, but adaptive locomotive behavior exists in the absence of neurons as well. For example, there is evidence that the movement of the multicellular body of certain slime molds, such as *Dictyostelium* ("social amoeba"), results from a difference in activity between the anterior and posterior cells (Bonner, 2008). *Dictyostelium* can respond to minute variations of light, temperature, and concentrations of ammonia and oxygen. In many cases it is known that these stimuli affect the relative location of so-called "organizer cells", which release a diffusive chemical signal, the same signal used during the aggregation of single cells into the body (reviewed in Kessin, 2001). The relative location of these organizers controls the activity level of the cells across the body, which in turn controls the direction of motion. This impressive capacity of *Dictyostelium* for effective and reactive behavior occurs without any nerve cells.

Dictyostelium is one of the most important "model organisms" in biology for the study of development because its structure is simple and the number of cell types limited. The assumption that knowledge about complex biological systems can be gained by first studying simpler organisms has proven tremendously successful. We share this view and, in the present work, propose that in order to study body-brain co-development more effectively, it is helpful to consider the basic case of a body devoid of any nervous system. Our approach is related to the investigation of minimal sets of behaviors that can still exhibit interesting "cognitive" abilities (*minimal cognition*; Beer, 1996). In this context, animats capable of executing non-trivial tasks are generated and tested on some cognitive challenge. For example, Dale and Husbands (2009) describe a 1D animat that can perform shape discrimination with limited memory, using only a reaction-diffusion system. Such systems are known to model many developmental processes (Yamada et al., 2007; Lefèvre and Mangin, 2010), hence this choice is consistent with the view that regulation of development and regulation of behavior have mechanisms in common.

The present work brings several new aspects to the discussion of the relations between behavior and development, minimal cognition, and brain-body co-evolution. First, we achieve an important step towards minimal cognition, namely the coordinated behavior of multiple cells, based on a biologically plausible model of gene regulatory networks (GRNs). Second, we utilize the same instance of GRN for both developmental and behavioral control. Our experiments rely on a modeling and simulation platform called GReaNs (for *Genetic Regulatory evolving artificial Networks*), which is dedicated to the study of GRN evolution and evolutionary development based on a linear genomic representation of GRNs. Two of us (Joachimczak and Wróbel, 2011) have shown previously that GReaNs was successful at evolving asymmetrical multicellular structures displaying asymmetrical patterning. We then applied the same model of GRNs to signal processing (Joachimczak and Wróbel, 2010b) and to directing the motion of unicellular animats (Joachimczak and Wróbel, 2010a). In the present work, we rely on another recent extension of GReaNs (Joachimczak and Wróbel, 2012) to model soft-bodied multicellular animats in motion.

On the spectrum of available developmental and generative systems, the GReaNs platform belongs to a relatively small family of models that attempt to retain some degree of "biological realism" (e.g., among others, Mjolsness et al., 1991; Hogeweg, 2000; Salazar-Ciudad and Jernvall, 2002; Doursat, 2008). From the viewpoint of artificial life, these models belong to the "cell chemistry" approaches identified by Stanley and Miikkulainen (2003) in their taxonomic review of artificial embryogeny research. They all attempt to combine the essential chemical and physical principles of both genetic regulation *and* cellular mechanics, and to form fine-grained agent-based modeling rules based on these principles. In such models, the final shape and behavior of an organism are the result of complex interactions taking place at several scales of abstraction. Generally, at the smallest scale, each cell contains a genome that codes for gene products and regulatory sites, and whose interactions (based on sequence-matching in GReaNs) can be mapped to a GRN. On a mesoscopic level, the continuous, dynamic update of product concentrations in the cells leads to various types of cell behavior, such as division and differentiation, as products in the genome build up or degrade over time. Finally, the macroscopic shape and action of the organism emerges from the physical interactions between neighboring cells, which move in space during growth and motion.

In this study, we introduce in the GReaNs model the possibility that global patterns of cell activity—themselves the product of interactions between controller cells, the physical structure of the individual, and the properties of the simulated environment—give rise to the movement of developed multicellular bodies. We show that the control and coordination of this movement do not require an artificial nervous system, but can merely be achieved by decentralized GRN activity in every cell and signal diffusion.

A model of development, behavior and evolution of soft-bodied animats

Genome and GRN

The integrated model of genome, GRN, development and evolution presented in this paper is essentially the same as our recent extension of GReaNs that modeled soft-bodied multicellular animats in motion (Joachimczak and Wróbel, 2012). For the sake of completeness, however, we provide here a full description of the model. The main difference is that, in the experiments shown here, the GRN continues to function during animat movement, while in the previous version the GRN dynamics stopped at the end of development and its final outputs specified the oscillatory behavior of the cells.

A genome in GReaNs is composed of genetic modules or "elements", which are ordered sets of numbers and belong to three different classes (Fig. 1): G elements code for regulatory products/factors, an abstraction of the biological transcription factors and diffusive products; P elements are regulatory regions that control (promote or repress) the expression of G elements; and S elements are used as inputs into, and outputs from, the network.

A linear genome is parsed sequentially to build a GRN in which nodes correspond to *regulatory units*. A regulatory unit is a contiguous series of P elements followed by a contiguous series of G elements in the genome. The factors coded by G elements belonging to one unit have the same concentration. As for S elements, they are each mapped to a separate node: when the S element corresponds to an input—to a node with only one regulatory factor (an input factor), when it corresponds to an output—to a node with one regulatory region and one product (an output factor). Output factors determine the actions performed by the cell but do not have affinity to regulatory regions. Products coded by G elements can have affinity to P elements or regulatory regions in output nodes. Factors coded by input S elements can only have affinity to P elements.

The internal structure of each genetic element is composed of several fields (Fig. 1): a *type* field, which specifies the exact type of the element (subtype of G, P or S); a *sign* field; and *coordinate* fields which specify a point in $\mathbb{R}^N$ space (here $N = 2$). The affinity between a regulatory factor and a regulatory region is a decreasing exponential function of the Euclidean distance between their 2D points (weight reaches maximum 10 when points overlap), with a cutoff value to prevent full connectivity (weight is 0 when points are too far apart). The sign of the weight (and thus if it contributes to inhibition or excitation) is determined by multiplying the *sign* fields of the respective elements. Since one regulatory unit of the GRN can be composed of multiple P and G elements, any two nodes in the graph can be connected together through multiple edges. There is no limit on the size of the GRN (number of nodes) in GReaNs.

The concentrations of factors are updated in discrete time steps. First, the activation level of each regulatory region of a node is defined as the weighted sum of the concentrations of all factors (possibly from other units) that have a non-zero affinity to it. If the node corresponds to a regulatory unit, the activation of all P elements of a unit is summed. The rate at which the concentration of factors of a node change is determined using the following update rule:

$$\Delta L = (\tanh \frac{A}{2} - L)\Delta t \tag{1}$$

where Δt (the integration time step) determines how fast the factors accumulate or degrade in relation to the simulation time step (the value 0.05 is used in this paper), L is the current concentration of the factors in the node (if there is more than one, all have the same concentration), restricted to the interval $[0, 1)$, and A is the summed activation of all P elements in the unit (the effect of a product on a promoter is calculated by multiplying the product's concentration by the weight).

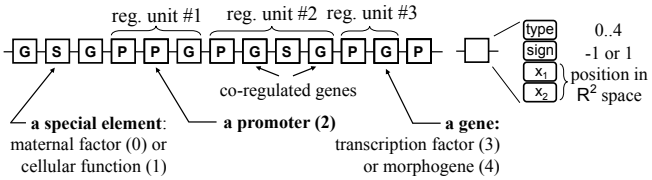

Figure 1: Genome and structure of a single genetic element. Each element consists of a *type* field, which specifies the class of the element (G, P or S), a *sign* field, and a sequence of N abstract *coordinates* in $\mathbb{R}^N$ space ($N = 2$ here), which determine its affinity to other elements.

The S elements of the genome are used to code for GRN inputs and outputs, which provide to a cell certain external signals and the ability to perform certain actions. The concentration of input factors is determined outside of the cell and they diffuse in the physical space of the developmental process (here, in 2D). They can be seen as playing the role of "maternal morphogens". We used here four different input factors, three of which were produced by sources at specific locations. The fourth factor had a uniform concentration of 1 across the entire space.

Outputs correspond here to six possible cellular actions. The first four actions—cell division, change in cell orientation (rotation to the left and to the right), and change in cell size—affect only development, while the other two actions—coding for cell contraction and expansion—affect only the physical motion of the multicellular animat.

Developmental process

The developmental process starts from a single cell. Each cell contains a copy of the genome, which encodes the GRN and whose activity controls the cell's developmental behavior. This behavior comprises mechanical rules and chemical rules, which are coupled and influence each other.

Mechanical rules: Cells occupy real-valued positions in 2D space (Fig. 2). An embryo develops in a simulated fluid-like environment, in which cells behave as soft (non-rigid) physical objects. The overall structure of the embryo is maintained by elastic forces between nearest-neighbor cells. Forces are repulsive when cells are too close and attractive otherwise, reaching an optimal distance at equilibrium. After each division of a mother cell, the two daughter cells partially overlap (see rotation action below), so they immediately repel each other.

Chemical rules: Exogenous maternal morphogens located in the environment allow differentiation based on cells' location in space. Cells also produce endogenous diffusive factors that affect morphogenesis (morphogens). In the simplified, grid-less diffusion model used here, the concentration of these regulatory factors in a cell at a given location is a function of the distance from the source and (for endogenous factors) the historical concentration in the source cells.

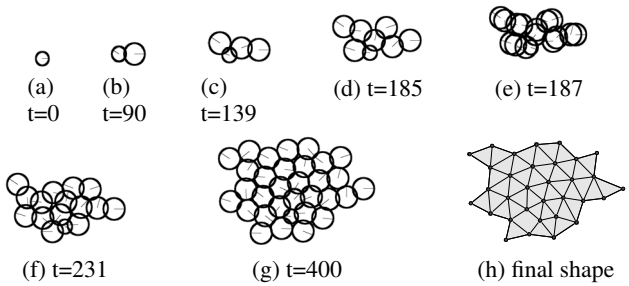

Figure 2: Example of the developmental mechanics. Cells are represented as circles. In (e), cells have just divided but elastic forces have not yet pushed them apart. This was achieved in (f). (h) shows the final structure after cells were connected with springs, see Fig. 4a for the same animat in motion.

Mechanical-chemical coupling: We describe the first four output functions mentioned above. *Cell division* is triggered when the concentration buildup of a specific "division factor" (coded by one of the S elements) reaches a threshold of 0.9. Should this element become disconnected from the GRN (due to mutation) or lost (due to deletion), the individual would consist of a single cell and have zero fitness. The division is asymmetric: a new "daughter" cell is formed from a given "mother" cell. In this paper, there is no asymmetry in the distribution of gene products (the daughter inherits all the concentrations from the mother), but rather in the cell's size and orientation angle. This angle is an abstraction of the cell's polarization axis and/or cleavage plane and determines where the daughter cell is placed with respect to the mother. The orientation of the mother cell remains the same after division, while *cell rotation* factors change the daughter cell's angle proportionally to their concentration. A "right rotation factor" causes an increase of the angle, while a "left rotation factor" causes its decrease (a $\pm 2\pi$ rotation corresponds to the maximum concentration 1 of the right/left factor). Finally, *size increase* determines the radius of the daughter cell at division, which may be up to 1.5 times the default radius when the concentration of the corresponding "size factor" is at the maximum of 1.

Final structure

The developmental phase is followed by a transformation of the obtained morphology into the actual structure of the animat (Fig. 3). In principle, this transformation restricts the set of evolvable structures, but it is also a way to keep the evolutionary search focused, provided that such restriction is still able to produce individuals that are diverse and relevant to the challenge at hand.

The first step of the transformation process consists of outlining a tight, but not necessarily convex, hull that encloses all the cells. This requires identifying the "outer" cells and connecting the centers of adjacent cells with edges,

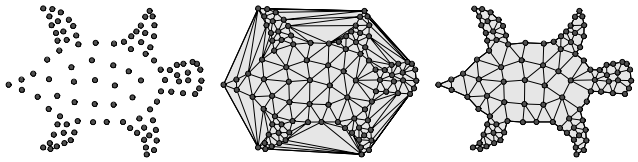

(a) (b) (c)

Figure 3: Algorithmic transformation of a set of points into an animat structure: (a) cell centers at the end of the developmental phase, (b) Delaunay triangulation of the set, (c) Gabriel graph of the set (final structure).

while preserving "concave" regions. The resulting hull corresponds to the external surface or "skin" of the animat's body, which in a simulated fluid-like environment is the only source of drag forces. In a second step, the animat's internal structure is completed by connecting all the remaining neighboring cells through elastic edges modeled as damped springs. This structural graph is calculated on the basis of cells' centers only. Cells' radii affect the final structure only implicitly, by determining the equilibrium positions of the cells during development.

To calculate connectivity, we use a particular notion of spatial proximity defined by the *Gabriel graph* (Gabriel and Sokal, 1969), which is different from nearest neighbors: any two points will be connected by an edge if and only if there are no other points inside the circle whose diameter is that edge. The Gabriel graph is a convenient way to obtain non-convex hulls: it is non-parameterized, scale invariant, and relatively straightforward to compute. Because it is a subgraph of the Delaunay triangulation, it can be derived from the latter in linear time by removing all the edges that do not fulfill the above proximity criterion.

Motion generation

The final structure of the animat defines a soft body consisting of springs (the edges of the Gabriel graph), masses (the cells, vertices of the graph), and pressurized chambers (the polygons formed by the edges). We employed the Bullet library (2011), but since it was originally created to simulate rigid-body objects, forces affecting the soft-bodied animats were calculated by custom GReaNs code while the Bullet library was only used to integrate the motion of cell centers.

All cells have the same mass, and all edges have the same elasticity and damping coefficients (Hook's coefficients). Actuation is achieved by varying the resting lengths of the springs in the structural graph. Each cell-vertex can contract or expand the elastic edges that are connected to it, provoking the shrinkage or dilation of the regions around that cell. A cell can control this process using two outputs of its GRN: one output for the contraction of the resting lengths, the other output for their expansion. Together, two cells connected by an edge modify the resting length L of that edge additively:

$$L = (1 + A_{max} \cdot (e_1 + e_2 - c_1 - c_2)) \cdot L_0 \qquad (2)$$

where e_1, e_2 (respectively, c_1, c_2) are the concentration levels of the expansion (respectively, contraction) factors in the two cells, and A_{max} is a parameter of the system representing the maximum actuation amplitude (set to 0.2 here).

Additionally, a mechanism of *pressurized chambers* is introduced in the body to oppose excessive compression and prevent collisions of internal nodes with springs. These chambers play the role of a "hydrostatic skeleton" for the animat. At the time of the transformation to the final structure, the area of each chamber is computed and defined as its equilibrium area. Then, as a chamber shrinks or expands during movement, pressure forces react along the normal of each one of its edges:

$$F_p = c_p \cdot L \cdot (1 - \frac{S}{S_0}) \qquad (3)$$

where F_p is the pressure force acting outward along the normal of the edge that is considered, L is the length of this edge, S and S_0 represent the current and equilibrium areas of the chamber, and c_p is a global pressure coefficient controlling the resistance to compression.

To simulate the fluid-like environment, we apply the simplified model of fluid drag described by Sfakiotakis and Tsakiris (2006) and previously used in a work about developing spring-mass animats by Schramm et al. (2011). This model assumes that the fluid is stationary and that the force acting on a single edge of the skin is a sum of tangential and normal drag components, v_T and v_N, with respect to the motion of this edge:

$$F_T = -d_T \cdot L \cdot \mathrm{sign}(v_T) \cdot (v_T)^2 \qquad (4)$$

$$F_N = -d_N \cdot L \cdot \mathrm{sign}(v_N) \cdot (v_N)^2 \qquad (5)$$

where d_T and d_N are the fluid drag coefficients (here, $d_N = 200 d_T$). Since animats are soft-bodied, the lengths of the springs change dynamically and the direction of motion of a given edge is defined as the direction of its center.

Genetic algorithm and fitness evaluation

We use here essentially the same genetic algorithm as in our previous work (Joachimczak and Wróbel, 2012), with constant population size (300), elitism, tournament selection and multipoint crossover for sexual reproduction (concerning 20% of the individuals at each generation). In GReaNs, genetic operators act at the level of the genomic elements (affecting element types, sign bits, and coordinates) and multiple elements (duplications, deletions, and crossover).

To assess the fitness, the genome is first transformed into a GRN. If the GRN does not contain a directed path (sequence of connected nodes) from at least one input element to the

output elements corresponding to cell division and animat actuation, the individual is assigned a zero fitness (it would be motionless). The development is allowed to proceed for 400 simulation steps. Cell division is terminated when the size of the embryo reaches 32 cells. Individuals containing less than three cells and individuals whose development process includes a cell division in the last 100 simulation steps of their development are assigned a zero fitness. The purpose of the latter criterion is to allow time for the morphology to equilibrate after the last cell division.

After the transformation into a soft-bodied animat, the multicellular body is immersed in the simulated physical world and allowed to equilibrate for 200 simulation steps while the GRN is stopped. This equilibration step is necessary because the levels of expansion and contraction factors in each cell at the end of development can be non-zero. Then, the GRN is started again and the animat is allowed to move for 6000 simulation steps, at the end of which the distance traveled by its center of mass is converted into a fitness value. Since absolute distance is rewarded, it is beneficial for individuals to be bigger. Indeed, we observe that the best evolved animats almost always have the maximum possible cell size and number (32 cells). The rules of physics in the environment used for development and assessment of mobility are different, but the cells can still communicate through diffusive factors during motion. This diffusion process takes into account distances between cells at the end of development.

The initial population is generated randomly, by creating positive-fitness individuals with 10 regulatory units, each unit containing one P and one G element. Most random genomes created in this fashion have a zero fitness, so it is necessary to generate a few hundred of them before a positive-fitness individual can be placed in the initial population.

Results and Analysis

We have simulated evolution in several independent runs under various environmental conditions (the physics parameters for the simulation of motion, see below). We avoided settings in which the mass of the cells was so high that it could result in exaggerated stretch to the body, or in which spring constants were so high that they would lead to instability or "unnatural" motions. Unnatural motions exploit unwanted artifacts, such as collisions of internal nodes with each other or interpenetration of body fragments (the latter could always be reduced by decreasing the time step). Under these constraints, we were still able to obtain effective patterns of locomotion over two orders of magnitude of the fluid drag coefficient d_N, and across a range of Hook's elastic coefficients and hydrostatic skeleton pressure values c_p.

Evolution was successful at finding animats capable of locomotion. In nearly all runs, using a variety of parameters for the local physics, our genetic algorithm produced GRNs that could control both a developing animat morphology and its functional motion via coordinated contractions and expansions. In some evolutionary runs, structures that looked like "appendages" have emerged. Motion was caused by emergent oscillations and other periodic patterns controlled by the GRN in each individual cell of the animat. The results obtained here are consistent with our previous experiments in which motion was not dynamically controlled by the GRN in real time, but rather the equilibrium length of the springs and the phase and frequency of oscillations were determined and fixed at the end of development (Joachimczak and Wróbel, 2012).

To analyze the behavior of the animats, we describe them over two axes: the main body axis (front-back) and the left-right axis. These were determined by computing the direction of motion of the animat, and declaring the resulting vector (extending from the center of mass of the animat) as the main body axis, then the orthogonal direction as the left-right axis. The *activity* of each cell was defined as the absolute change in contraction or expansion of the resting length from the previous time step ($|\Delta(e_i - c_i)|$ from equation 2). The average activity along an axis was computed by projecting all cells onto this axis, and calculating the mean over the area before and after the center of mass. We will thus discuss the average cell activity of the front of the animat compared to the back, and the left compared to the right. We also show the concentrations of the expansion and contraction factors in a few selected cells of the animats, to explain how overall animat motion is generated by the collective behavior of several GRNs.

We identified several distinct strategies through which locomotion was achieved. We informally describe four such strategies here, calling them *turtle*, *shark*, *worm*, and *jellyfish*.[1] Naturally, these metaphors only refer to the visual appearance of motion, not the actual mechanism by which these real-world, nerve-endowed animals operate. Indeed, the difficulty of finding nerve-free organisms for such metaphors highlights the fact that the biological organisms that we are familiar with control their motion using nervous systems. The *worms* and *turtles* are similar to individuals seen in our previous work (Joachimczak and Wróbel, 2012). The *jellyfish* strategy, however, is new in our present control model, and the *shark* is either new or, perhaps, an extreme version of a worm-like behavior.

The *turtle* strategy is based on the use of approximately symmetric protrusions on the left and right of the animat, which move in more or less regular oscillatory patterns. Average cell activity oscillate symmetrically over the left-right axis, with changes in phase and amplitude over the front-back axis. Similar individuals constituted the majority of the best individuals obtained in independent runs under low fluid drag. In most of these individuals, the motion stemmed

[1] Supplementary videos of animat behaviors are available at: `http://evosys.org/grnanimats`

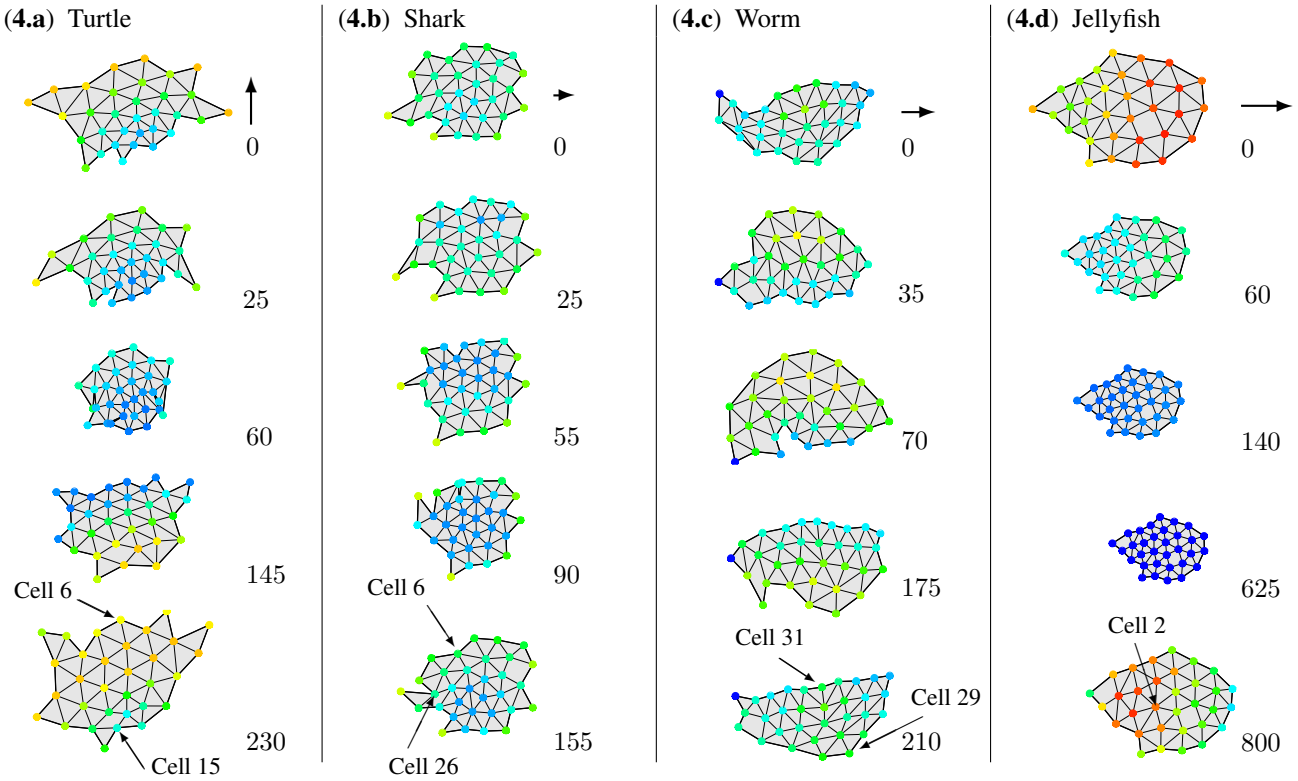

(4.1) A snapshot of motion cycles of the individuals. Node color indicates whether the cell is contracting or expanding its springs (red: expansion, blue: contraction, green: neutral). Numbers indicate the time steps in the cycle. The arrow is an approximation of the distance traveled by the center of mass in one cycle for each animat.

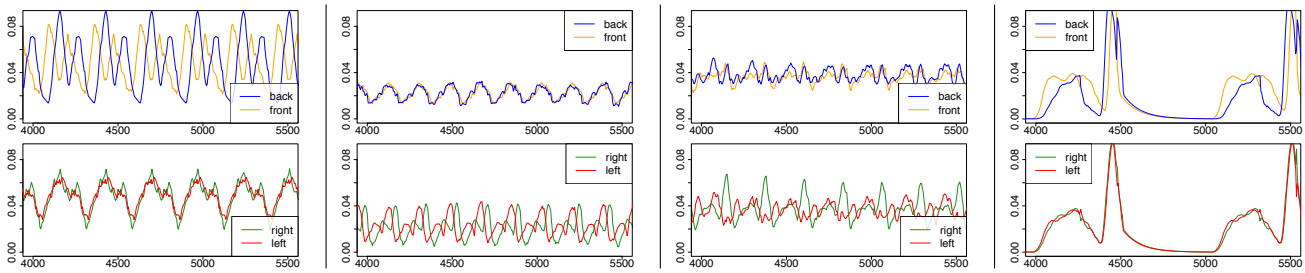

(4.2) Plots of the average activity of cells (*y-axis*) over time (*x-axis*) along the front-back and left-right axes of the animats.

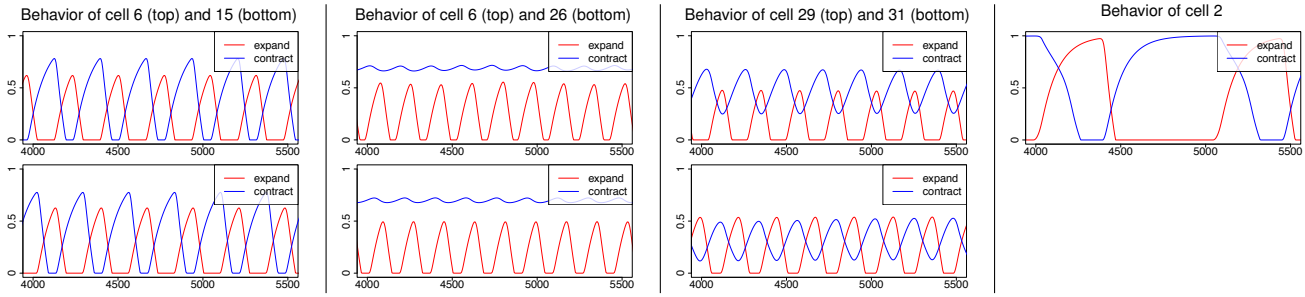

(4.3) Plots of pattern of actuation (*y-axis*) for one or two particular cells over time (*x-axis*), where the red line indicates the concentration of the expansion factor and the blue line corresponds to the contraction factor.

Figure 4: Visualization of exemplars of the four strategies of behavior discovered by evolution.

from a wave of expansions and contractions continuously traveling from the back towards the front of the animat. The analysis of one such individual (Fig. 4.a) revealed that cells shared the same overall evolved pattern of activity. The concentration of the factors that caused expansion and contraction remained antisynchronized inside each individual cell, while there was another phase shift (almost at antiphase) when comparing the same product between different cells in the front and the back of the animat (Fig. 4.3a). Thus contractions in the front practically corresponded to expansions in the back, and vice-versa (Fig. 4.2a, top), in a manner consistent with a traveling wave of contraction-expansion across the body.

In the *shark* strategy, there was a protrusion at the back of the animat, which oscillated at a relatively high frequency with a larger displacement than the remainder of the body. The average cell activity over the front-back axis oscillated symmetrically, while there was a change in phase over the left-right axis (Fig. 4.2b). Multiple individuals of this type have been observed, even though they clearly did not exhibit an aerodynamic shape. For the individual shown in Fig. 4b, the motion was driven by a wave of expansion that traveled in the direction perpendicular to the motion, from the left to the right. However, a cell located at the tip of the motion-generating protrusion was excluded from this wave pattern and maintained a constant maximum concentration of the expansion factor, thereby sustaining the length of protrusion. Furthermore, a bulge located on the left, next to the back protrusion, collided during its own expansion with the "tail" in every cycle, passing on its kinetic energy and making the tail quickly reverse its direction of motion. Interestingly, the concentration of the contraction factor remained constant (although not uniform) in all cells, so it only provided a bias for the resting lengths of the springs. The analysis of two particular cells located at the back of the individual (Fig. 4.3b) revealed sinusoidal oscillations of the expansion factor. They had the highest oscillation frequency among all individuals investigated in this paper.

The *worm* strategy involved an elongated body driven by the propagation of synchronized waves of contraction and expansion, which traveled in the direction perpendicular to the motion, from the left side of the body to the right, resulting in undulatory movement. Cell activity here was not symmetric, neither over the front-back nor over the left-right axis, and the average activity was less regular than in other strategies (Fig. 4.2c). Only a few such individuals were observed. Comparing the activity of the expansion and contraction factors in cells located symmetrically on the left and right sides of the body (Fig. 4.3c) revealed sinusoidal oscillations in antiphase and shifted approximately by half a period between the sides of the body.

Finally, animats using the fourth strategy, *jellyfish*, were bilaterally symmetric with one blunt end and one pointed end. The whole body expanded or contracted at the same time. Because fluid drag generated by an edge was proportional to the square of its velocity, slower expansion resulted in a smaller drag. Animats with a pointy front contracted slowly and expanded very rapidly, while animats with a pointy back expanded slowly and then contracted rapidly. In the individual of the latter type analyzed in detail (Fig. 4.2d), the compacted state was sustained and the body moved by inertia for some time, slowed down by the fluid drag, and then the cycle repeated itself. The overall impression was that of a propelling motion similar to a jellyfish. The observed pattern of cell activity resulted from the fact that the expansion factor's concentration decreased much faster than it increased (Fig. 4.3d), and from a matching dynamics of the contraction factor. The levels of both factors in the cell were stable when the body traveled by inertia.

Throughout, we noted that evolution found synchronized actuators for contraction and expansion to great effect. However, it seemed to avoid using the full amplitude of actuation possible. Rather, it explored a trade-off between amplitude and frequency: increasing the rate of activity buildup required more products binding at high levels to a given regulatory unit.

Summary

In this work, we have re-approached the development and control of virtual soft-bodied robots in GReaNs. In contrast to our previous study (Joachimczak and Wróbel, 2012) and other models (Schramm et al., 2011), the simulations described here relied on gene regulation for both the developmental process and behavioral control. Evolution was successful at generating moving animats and discovering several functional locomotion strategies. Motion was controlled via coordinated cell actions, where individual cells displayed emergent periodic patterns of expansion and contraction. Moreover, a previously unseen form of behavior, one characterized by rapid contraction or expansion of a largely symmetric animat, was discovered. This behavior was made possible by the GRN's fine-grained control over the contraction and expansion speeds, instead of a sine-driven actuation as in our previous work.

The reliance of the evolved locomotion mechanisms upon oscillatory changes in product concentrations is reminiscent of the rhythmic motor patterns of biological animals. By contrast, the movement of our animats is not based on a central pattern generator but a distributed collective effect. All cells of these soft-bodied, brainless animats can be potentially involved in actuation and control. It was demonstrated previously that a GRN could easily evolve toward an oscillatory behavior (e.g., Banzhaf, 2003; Joachimczak and Wróbel, 2010b). Our results show that, while motion relies on periodic changes of product concentration, development results in the differentiation of cells along the body axes in terms of phase and amplitude of these oscillations. In other terms, high evolvability stems from the relative ease of

evolving oscillatory GRNs, while a natural outcome of the developmental process is that neighboring cells have similar, though not identical dynamic properties.

The animat model used in this paper, a collection of springs modifying their resting length, is similar to a model of a soft-bodied robot. We expect that altering the physical part of the model to accommodate other types of actuation should yield similar results. In particular, the present system could be adjusted to generate designs for realistic soft-bodied robots. One of the possible directions for future work is to incorporate a notion of "energy efficiency" into the fitness function by assuming the use of a given type of existing hardware actuators.

Another direction for future work is to allow *active guidance* without a nervous system. This could be achieved for example by allowing surface cells to sense chemical gradients and modify their pattern of activity accordingly, as well as to pass information to internal cells through the use of diffusing morphogens.

One of the features of artificial life is the liberty to make counterfactual assumptions. Amongst other things, we view this work as a challenge to like-minded practitioners: qualitatively describe the role of neural machinery, and from there, refine our understanding of the role of a neural system.

Acknowledgments

This work was supported by a PAN-CNRS collaborative project, IO PAN (task IV.3), and a scholarship from the French government to BW. TK's and RD's positions at the ISC-PIF were funded by Région Ile-de-France. Computational resources were provided by the Polish Ministry of Science and Education (project N519 384236, N303 291234), the Tri-City Academic Computer Centre (TASK), and the Interdisciplinary Centre for Molecular and Mathematical Modeling (ICM, University of Warsaw; project G33-8).

References

Banzhaf, W. (2003). On the dynamics of an artificial regulatory network advances in artificial life. In *ECAL 2003: 7th European Conference on Artificial Life*, pages 217–227.

Beer, R. (1996). Toward the evolution of dynamical neural networks for minimally cognitive behavior. In *From animals to animats 4: International Conference on Simulation of Adaptive Behavior*, pages 421–429.

Bonner, J. T. (2008). *The Social Amoebae: The Biology of Cellular Slime Molds*. Princeton University Press.

Bullet Physics library 2.79 (2011). http://www.bulletphysics.org.

Dale, K. and Husbands, P. (2009). The evolution of reaction-diffusion controllers for minimally cognitive agents. *Artificial Life*, 16(1):1–19.

Doursat, R. (2008). Programmable architectures that are complex and self-organized: From morphogenesis to engineering. In *Artificial Life XI: Eleventh International Conference on the Simulation and Synthesis of Living Systems*, pages 181–188.

Gabriel, K. R. and Sokal, R. R. (1969). A new statistical approach to geographic variation analysis. *Systematic Zoology*, 18(3):259–278.

Hogeweg, P. (2000). Evolving mechanisms of morphogenesis: on the interplay between differential adhesion and cell differentiation. *Journal of Theoretical Biology*, 203(4):317–333.

Joachimczak, M. and Wróbel, B. (2010a). Evolving gene regulatory networks for real time control of foraging behaviours. In *Artificial Life XII: Twelfth International Conference on the Simulation and Synthesis of Living Systems*, pages 348–355.

Joachimczak, M. and Wróbel, B. (2010b). Processing signals with evolving artificial gene regulatory networks. In *Artificial Life XII: Twelfth International Conference on the Simulation and Synthesis of Living Systems*, pages 203–210.

Joachimczak, M. and Wróbel, B. (2011). Evolution of the morphology and patterning of artificial embryos: scaling the tricolour problem to the third dimension. In *ECAL 2009: 10th European Conference on Artificial Life*, pages 33–41.

Joachimczak, M. and Wróbel, B. (2012). Co-evolution of morphology and control of soft-bodied multicellular animats. In *GECCO '12: Proceedings of the 14th Annual Conference on Genetic and Evolutionary Computation*. ACM. (in print).

Kessin, R. (2001). *Dictyostelium: Evolution, Cell Biology, and the Development of Multicellularity*. Cambridge University Press.

Lefèvre, J. and Mangin, J.-F. (2010). A reaction-diffusion model of human brain development. *PLoS Computational Biology*, 6(4):e1000749+.

Mjolsness, E., Sharp, D. H., and Reinitz, J. (1991). A connectionist model of development. *Journal of Theoretical Biology*, 152(4):429–453.

Salazar-Ciudad, I. and Jernvall, J. (2002). A gene network model accounting for development and evolution of mammalian teeth. *Proceedings of the National Academy of Sciences*, 99(12):8116–8120.

Schramm, L., Jin, Y., and Sendhoff, B. (2011). Emerged coupling of motor control and morphological development in evolution of multi-cellular animats. In *ECAL 2009: 10th European Conference on Artificial Life*, pages 18–26.

Schramm, L. and Sendhoff, B. (2011). An animat's cell doctrine. In *ECAL 2011: 11th European Conference on the Synthesis and Simulation of Living Systems*, pages 739–746.

Sfakiotakis, M. and Tsakiris, D. P. (2006). SIMUUN : A simulation environment for undulatory locomotion. *International Journal of Modelling and Simulation*, 26:350–358.

Stanley, K. O. and Miikkulainen, R. (2003). A taxonomy for artificial embryogeny. *Artificial Life*, 9(2):93–130.

Yamada, H., Nakagaki, T., Baker, R. E., and Maini, P. K. (2007). Dispersion relation in oscillatory reaction-diffusion systems with self-consistent flow in true slime mold. *Journal of Mathematical Biology*, 54(6):745–760.